

Evidence of Abundant Stop Codon Readthrough in Drosophila and Other Metazoa

Irwin Jungreis^{1,2}, Michael F. Lin^{1,2}, Rebecca Spokony³, Clara S. Chan⁴, Nicolas Negre³, Alec Victorson³, Kevin P. White³, Manolis Kellis^{1,2,5}

¹MIT Computer Science and Artificial Intelligence Laboratory, Cambridge, Massachusetts 02139, USA; ²Broad Institute of MIT and Harvard, Cambridge, Massachusetts 02139, USA; ³Institute for Genomics and Systems Biology, University of Chicago, Chicago, IL 60637, USA. ⁴MIT Biology Department, Cambridge, Massachusetts 02139, USA.

⁵Corresponding author. E-mail manoli@mit.edu; fax 617-452-5034

Supplementary Figures:

Figure S1. Second ORF lengths. Fraction of in-frame second ORFs of given length (x axis) that are readthrough candidates (red), that show protein-coding constraint as indicated by positive PhyloCSF scores but with alternative plausible explanations (blue), or that have negative PhyloCSF score (green). Counts for each category indicated for each interval. Even among second ORFs greater than 100 amino-acids, only a quarter are readthrough candidates, highlighting the need for comparative evidence to distinguish them. Overall, 2% of second ORFs tested are readthrough candidates.

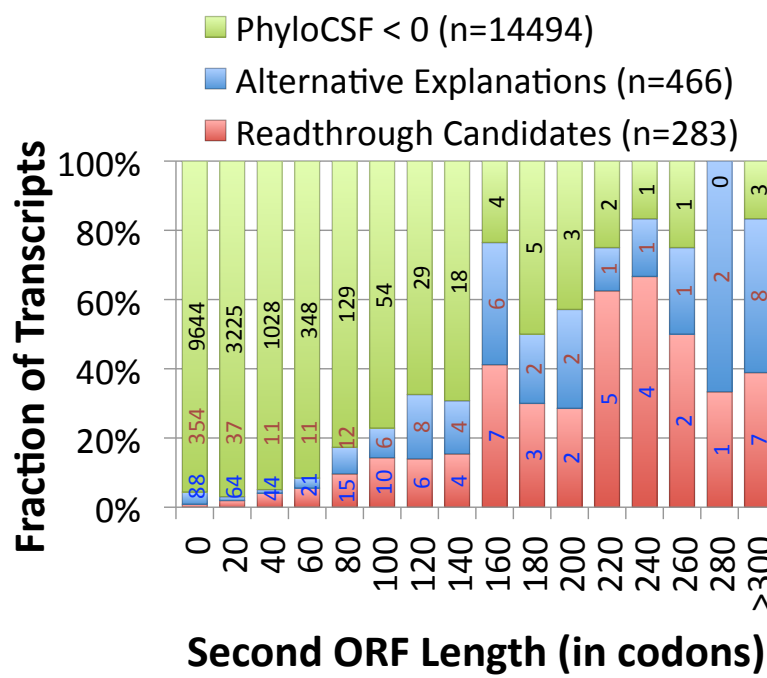


Figure S2. Periodic base pairing without smoothing. Identical to Figure 4C except without averaging sets of five consecutive codons. Although periodicity in the readthrough region is more difficult to discern visually without this smoothing, the pairing frequency at the third codon position remains higher than at the second position for almost all codons.

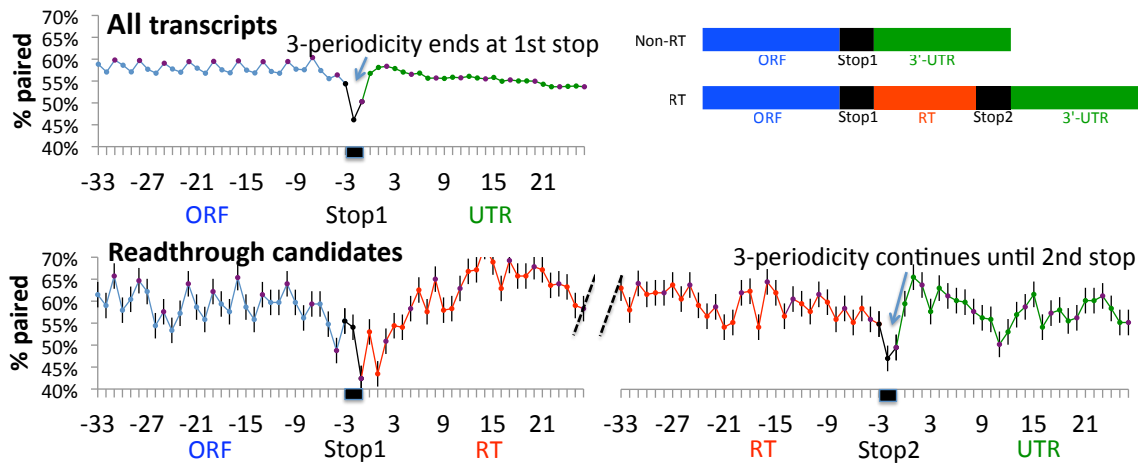


Figure S3. Close synonymous codons and ribosomal hopping. Distribution of distances (in bp) between the closest pair of synonymous in-frame codons bracketing the stop codon, for the readthrough candidates and for all transcripts. Error bars show Standard Error of Mean (SEM). The closest synonymous codons bracketing the stop codons of the readthrough candidates are not significantly closer than those of other transcripts, whereas we would expect them to be if ribosomal hopping was programmed in many of these transcripts.

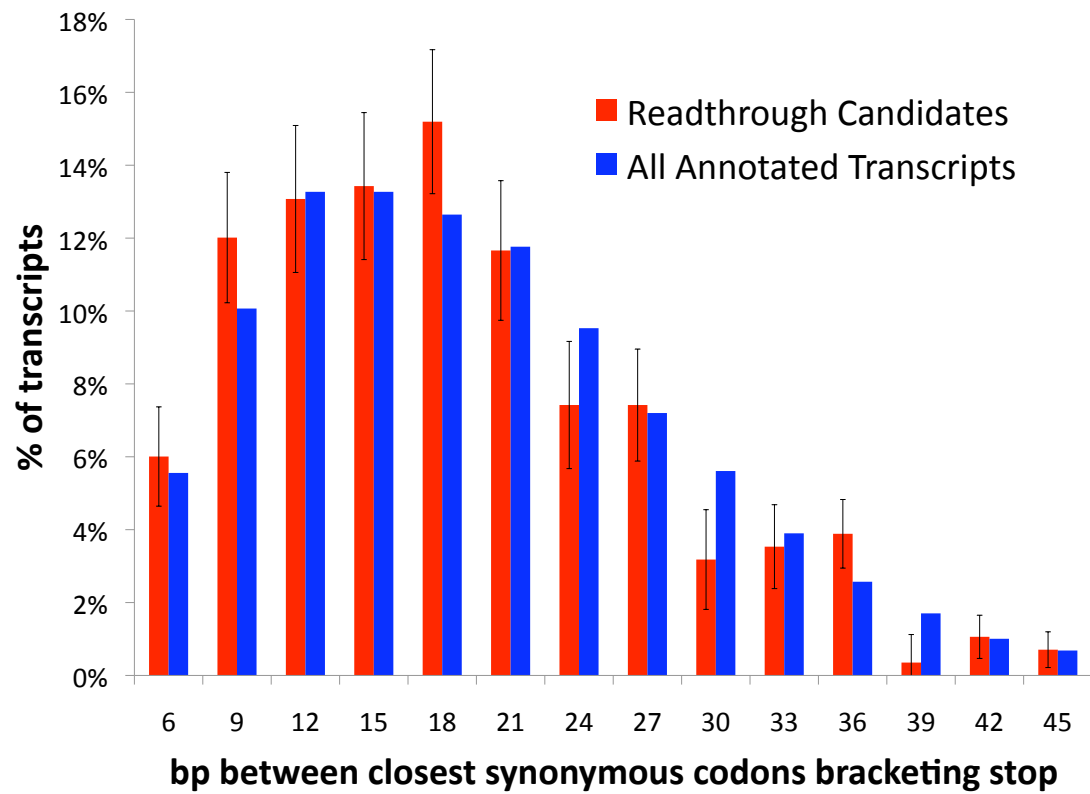


Figure S4. Stop codon context rules out splicing. The 4-base contexts are sorted in order of decreasing frequency among the 14,928 non-readthrough stop codons (blue). Context frequencies of the 1315 annotated "spliced-out-stops" (yellow), i.e., annotated stop codons that are within an intron of another annotated transcript of the same gene, are similar to those of the non-readthrough stop codons. Context frequencies for readthrough candidates (red) are opposite of non-readthrough transcripts and of *annotated* spliced-out-stops, whereas if the readthrough candidates were in fact *unannotated* spliced-out-stops we would expect their context frequencies to match those of the annotated ones, providing additional evidence that the evolutionary signatures of our readthrough candidates are not due to splicing.

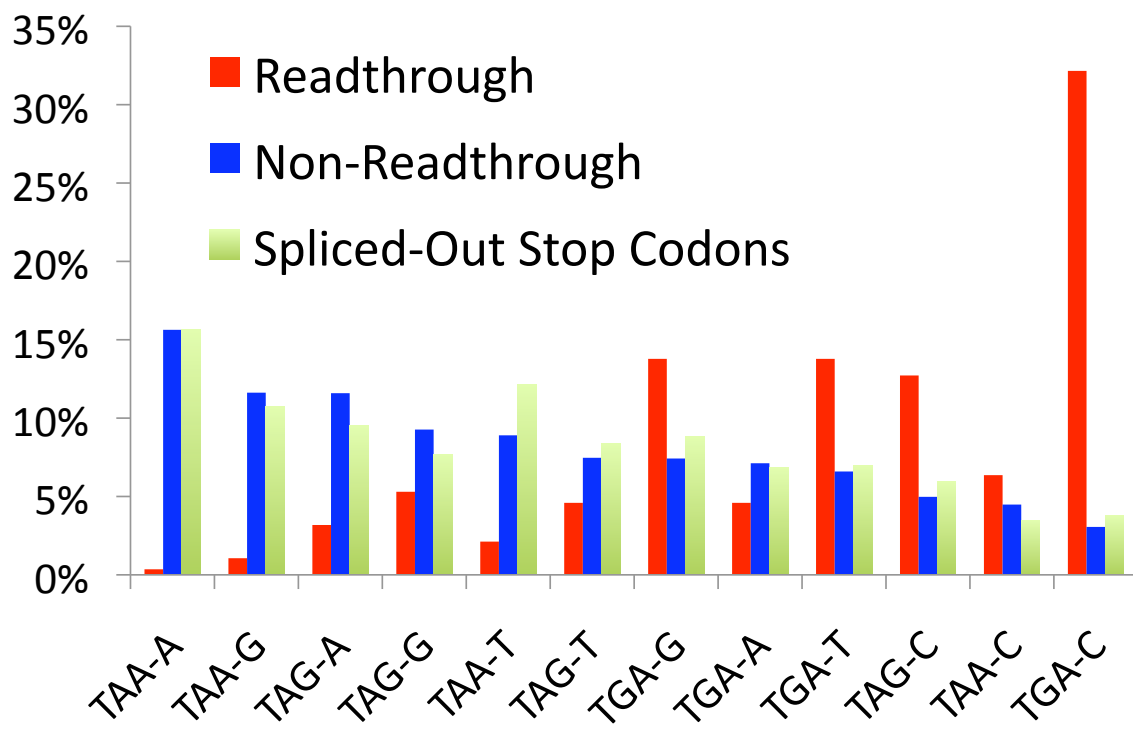


Figure S5. Length enrichments. Readthrough candidates as a group (red) show increased length (in nucleotides) and splicing complexity (number of transcript variants) compared to other transcripts (blue). Overall Length: sum of all introns, coding exons, and UTRs. Coding Length: length of first ORF. Adjusted 3'-UTR Length excludes second ORF for readthrough candidates. Splice Variants: number of annotated transcripts of the same gene. Numbers show actual size and bars denote size relative to non-readthrough genes. Error bars show standard error of mean (SEM) for readthrough candidates. Enrichments persist even after correcting for total intron length, 5'UTR length, 3'UTR length, or coding exon length (not shown).

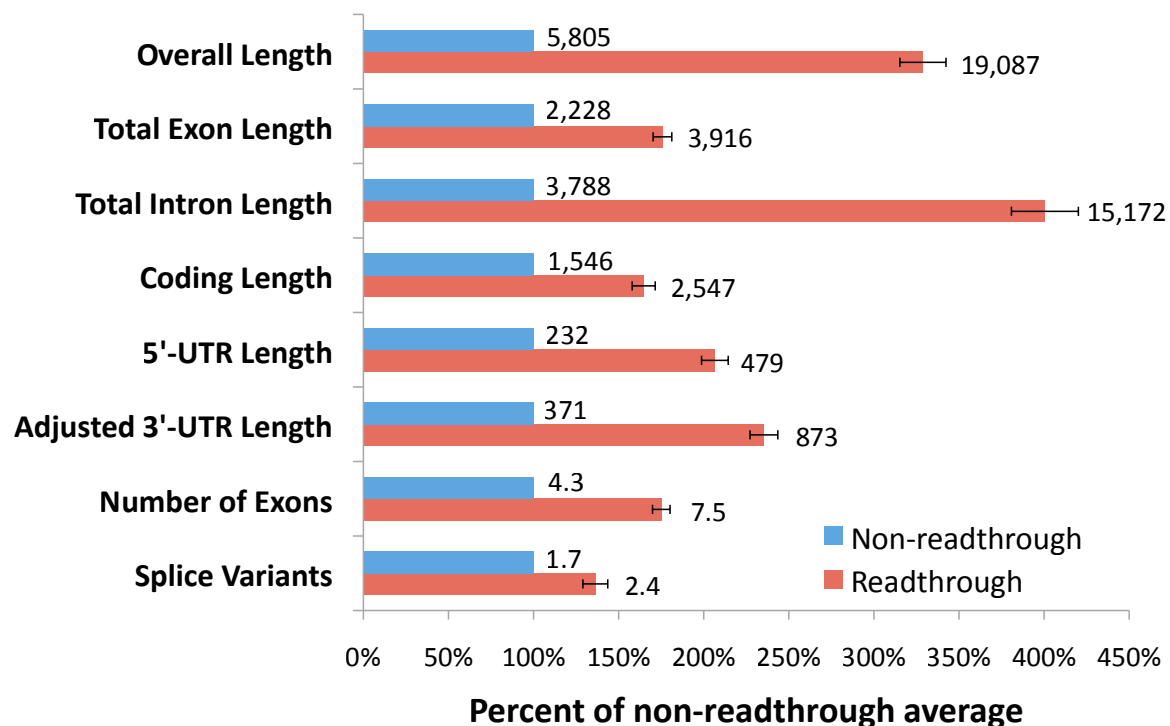


Figure S6. Unusual 1-, 2-, and 3-mer composition. Coding regions of readthrough candidates have unusual base composition and are enriched or depleted for some 2- and 3-mers.

Average frequency of bases and significant 2- and 3-mers in the coding regions of readthrough candidates (red), non-readthrough transcripts (blue), non-readthrough transcripts with similar primary transcript and UTR lengths to the readthrough candidates (yellow), and non-readthrough transcripts with similar base composition to the readthrough candidates (purple). The 2- and 3-mers shown are those for which the frequencies among readthrough candidates are significantly different from non-readthrough transcripts with similar base composition. Error bars show the Standard Error of Mean (*SEM*) of the readthrough candidates.

Correcting for the excess length of readthrough candidates decreases but does not remove the biases, and similarly, correcting for the high GC content of readthrough candidates decreases but does not remove the 2- and 3-mer biases.

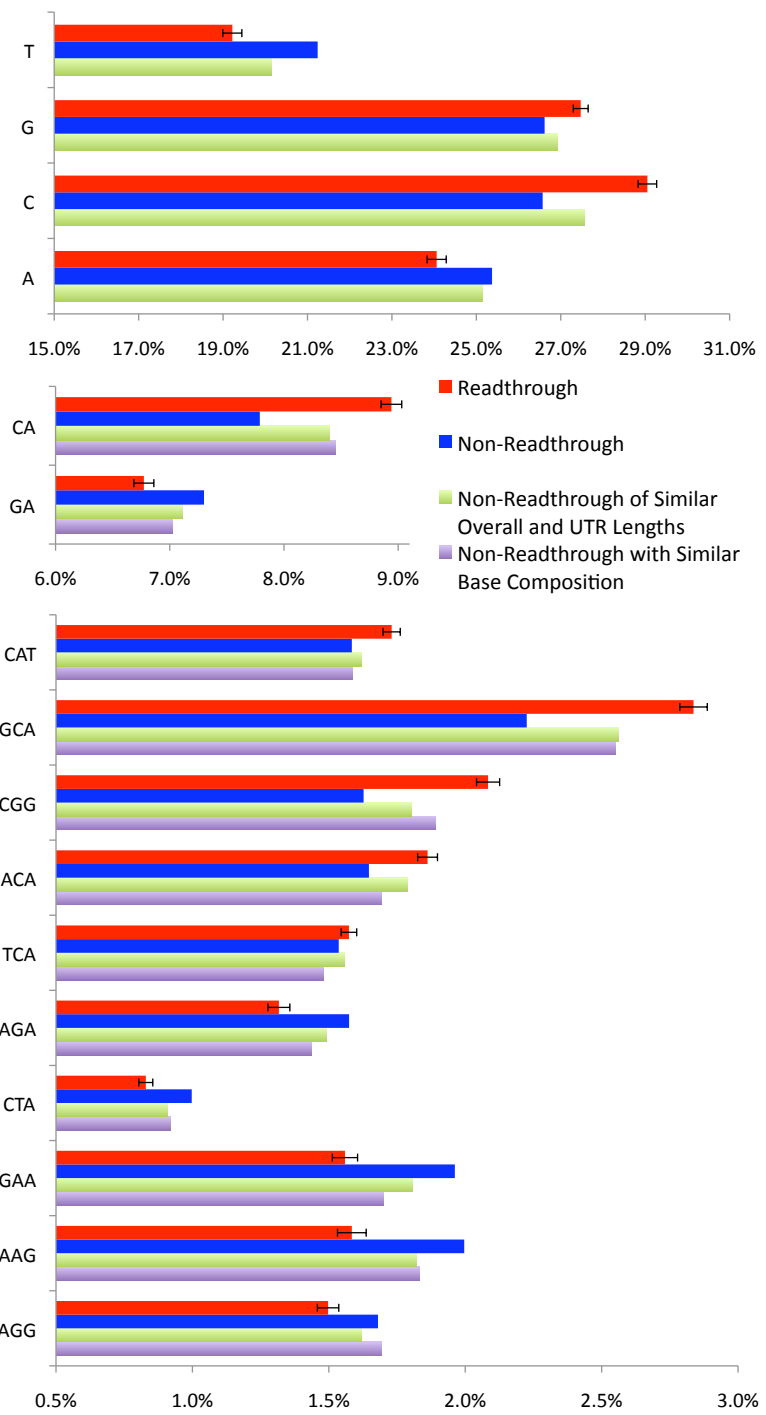


Figure S7. Length distribution biases may confound GO enrichment analysis. Distribution of total gene length (log scale) for readthrough candidates (red), non-readthrough transcripts (blue), and genes with the GO category "neurogenesis" (green), one of the most enriched among readthrough candidates. Readthrough candidates and neurogenesis genes have very similar length distribution, which would lead to artifactual enrichment if their above-average lengths are for independent reasons. Alternatively, since length could be an indication of more regulatory binding sites, it is possible that neurogenesis genes show increased regulation of many types, only one of which is readthrough.

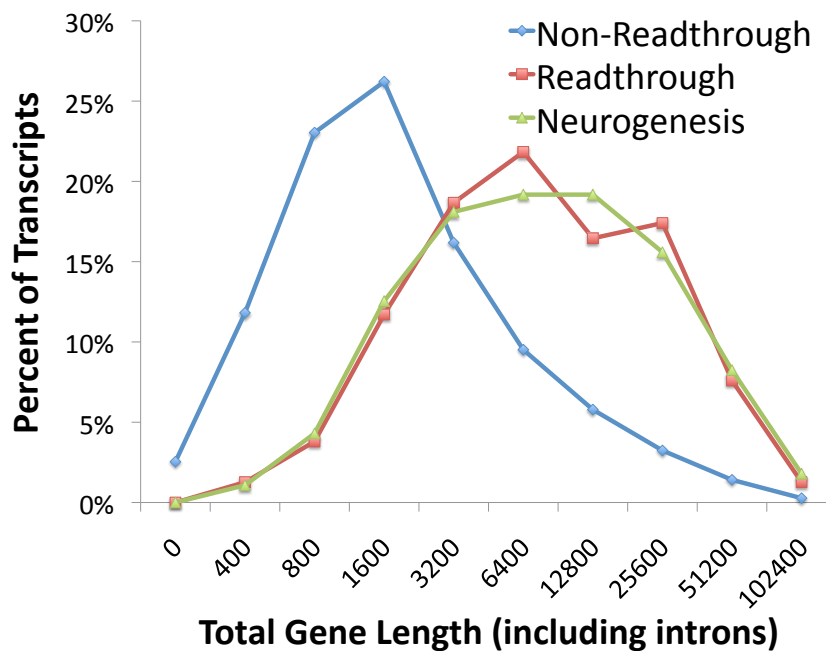


Figure S8. Enriched 8-mer. Readthrough regions and corresponding regions before the first stop are highly enriched for the 8-mer CAGCAGCA and long poly-Q repeats. (A) Fractions of readthrough candidates that include the 8-mer CAGCAGCA in readthrough regions, same length regions before the 1st stop (ORF), and same length regions after the second stop (3'-UTR), and the fractions of non-readthrough transcripts with this 8-mer in the regions before and after the 1st stop (region length for non-readthroughs chosen to match the length distribution of the readthrough regions). Readthrough candidates are highly enriched, both before and after the readthrough stop codon, compared to coding or non-coding regions of non-readthroughs. Most of the enrichment persists even among transcripts with similar base composition, or similar frequency of the 3-mer CAG or GCA (not shown). (B) Poly-Q length. Fraction of transcripts for which the specified region contains a sequence of consecutive Q codons of at least the specified length. The regions are the same as for (A). Many of the readthrough candidates have unusually long polyQ repeats either in the readthrough region or region before the 1st stop. The enrichment persists even if they are compared to non-readthroughs with similar frequency of the codon CAG (not shown). (C) Enrichment of 8-mer before the stop. The fraction of transcripts containing CAGCAGCA in 125-base windows before the first stop among readthrough candidates, non-readthrough transcripts, and non-readthroughs with similar frequencies of the 3-mers CAG, AGC, and GCA. The readthrough candidates are significantly enriched for the 8-mer in the last 250 nt before the stop codon, even relative to other transcripts with similar frequencies of these 3-mers. Enrichment of these 3-mers explains the enrichment of the 8-mer in the earlier 90% of the coding region, but not the excess enrichment near the 3' end.

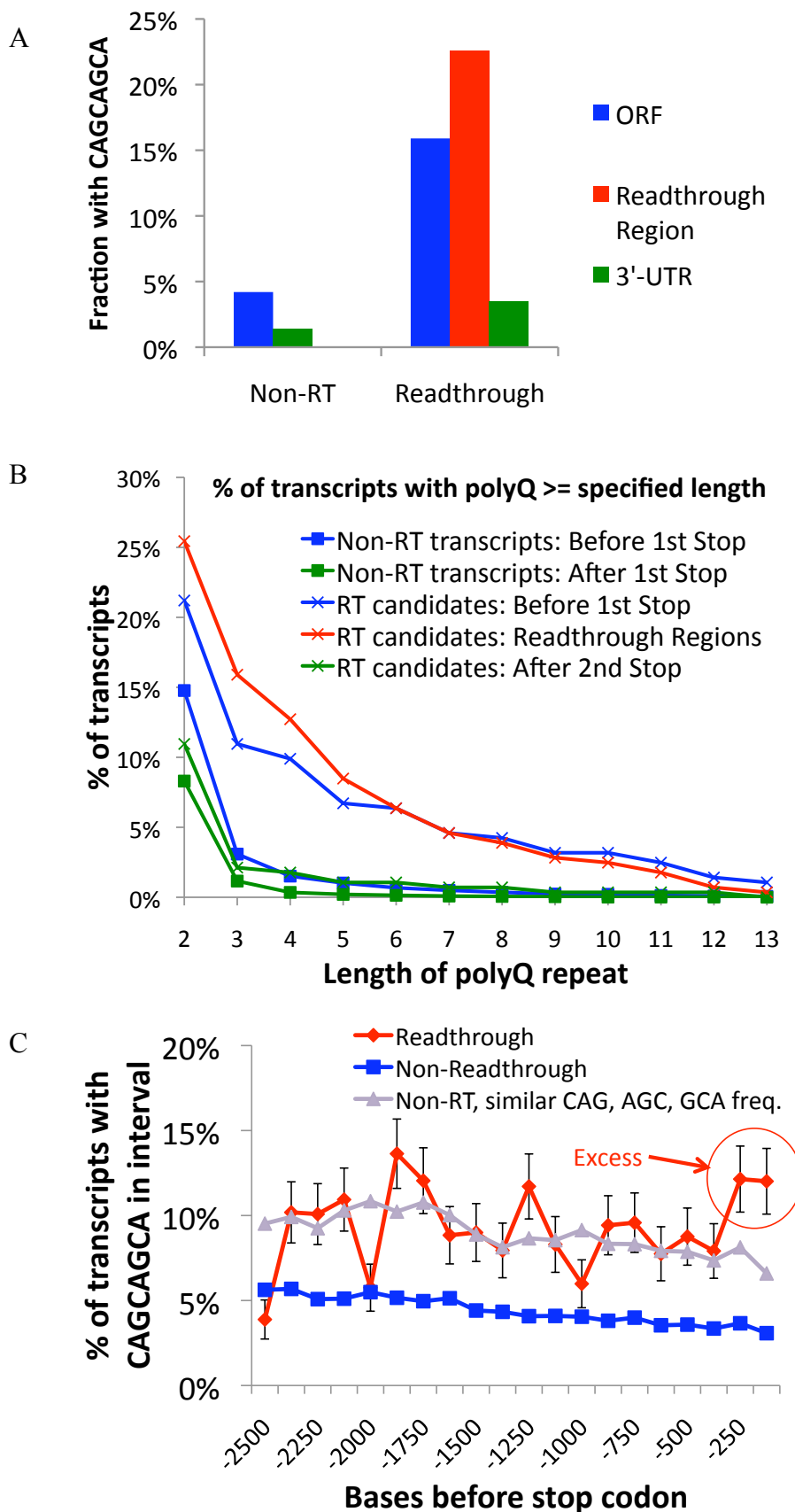
Figure S8. Enriched 8-mer.

Figure S9. Evolution by extension. Second ORF of *HLH4C*, one of our readthrough candidates that might have evolved by the extension scenario since the common ancestor of the 12 flies. Since second ORFs of genes that evolved this way will not be protein coding in some species, we would generally not expect to find them by our method, so they would not be readthrough candidates even if they are read through in *D. melanogaster*.

	E	T	P	X	D	N	A	G	A	S	S	F	A	T	S	C	S	F	S	E	A	M	F	F	A	P	P	X	E	V	G		
anc_aa																																	
ancestor	GAG	ACC	CCC	TGA	GAT	AAC	GCC	GGC	GCC	TCC	AGC	TTC	GCC	ACC	AGC	TGC	AGC	TTC	AGT	GAG	GCC	ATG	TTC	TTT	GCC	CCG	CCC	TAG	GAG	GTG	GGG		
dmel	GAG	ACC	CCC	TGA	GAT	AGG	GCC	GGC	GCC	TCC	AGT	TTC	GCC	ACC	AGC	TGC	CTC	TTC	AAU	GAG	GCC	AAT	TTC	TTC	GCC	CCC	TAG	GAG	GTG	GGG			
dsim	GAG	ACC	CCC	TGA	GAC	AGG	GCC	GGC	GCC	TCC	AGC	TTC	GCC	ACC	AGC	TGC	CTC	TTC	AAU	GAG	GCC	AAT	TTC	TTC	GCC	CCC	TAG	GAG	GTG	GGG			
dsec	GAG	ACC	CCC	TGA	GAC	AGG	GCC	GGC	GCC	TCC	AGC	TTC	GCC	ACC	AGC	TGC	CTC	TTC	AAU	GAG	GCC	AAT	TTC	ATC	GCC	CCC	TAG	GAG	GTG	GGG			
dyak	GAG	ACC	CCC	TGA	GAC	AGG	GCC	GGC	GGC	TTC	TCC	AGC	TTC	GCC	ACC	AGC	TGC	CTC	TTC	AAU	GAG	GCC	AAC	TTC	TTC	GCC	CCC	TAG	G--	-CG	TGG		
dere	GAG	ACC	CCC	TGA	GAC	AGG	GCC	GGG	GCC	TCC	AGC	TTC	GCC	ACC	AGT	TGC	CTC	TTC	AAU	GAG	GCC	AAT	TTC	TTC	GCC	CCC	TAG	GAG	GTG	GGG			
dana	GAG	ACC	CCC	TGA	GAC	AAC	GCC	GGG	SGA	TCC	AGC	TTC	GCC	ACC	AGC	TGC	ATC	TTC	AAU	GAG	GCC	AAC	TTC	TTT	GCA	CCG	CCC	TAG	GAT	G--	--		
dpse	GAG	ACC	CCC	TGA	GAT	AGT	GGT	AGC	GCC	TCT	AGC	TTC	AAU	ACC	AGC	TGC	AGT	GAG	GCC	ATG	TTC	TTT	GCA	CCA	CCA	TAG	GA				
dper	GAG	ACC	CCC	TGA	GAT	AGT	GGT	AGC	GCC	TCT	AGC	ATC	AAU	ACC	AGC	TGC	AGC	TTC	AGT	GAG	GCC	ATG	TTC	TTT	GCA	CCG	CCA	TAG	GA		
dwil	GAG	ACC	CCC	TGA	GAT	AAU	GCC	GGC	GGC	TCC	AGC	TTC	AAU	ACC	AGC	TGC	AGC	TTC	AGT	GAG	GCC	ATG	CTC	TTC	GCC	CAC	C	---	---	...			
avir	GAG	ACC	CCC	TGA	GAC	GGC	GGC	AAU	GCC	TCC	AGC	T--	GCA	GCC	AGT	TGC	C	---					
dmoj	GAG	ACC	CCC	TGA	GAT	AGC	GCC	AAU	GCC	TCC	AGC	T--	GCA	GCC	AGT	TGC	C	---						
dgri	GAG	ACA	CCC	TGA	GAC	GGC	GGC	AAU	GCC	TCC	AGC	T--	GCA	GCC	AGT	TGC	C	---	...	A	GGC	GCC	ATG	TTC	CTA	AC	CTT	CCC	TCG	---	...		

Figure S10. Rabbit beta-globin. Mammal alignment after the first stop codon for the known readthrough gene, rabbit beta-globin (some species not shown). The readthrough region in rabbit is not conserved, even compared to its closest relatives among the aligned species, so readthrough could be a species-specific event.

anc_aa	H	X	A	P	F	P	A	V	Q	F	L	G	K	A	P	L	S	P	E	P	N	Y	X	T	W	G	N	Y							
ancestor	CAC	TAA	GCT	CCC	TTT	CCT	GCT	GTC	CAA	TTC	CTA	GGA	AAG	GCC	CCT	TTG	TCC	CCA	GAG	GCC	AAC	TAC	TGA	ACA	TGG	GGA	AAT	TAT							
Human	CAC	TAA	GCT	CG	---	C	TTT	CTT	GCT	GT	-C	CAA	TTT	CTA	TTA	-	AAG	GTT	CCT	TTG	TTC	GCT	AAG	TCC	AAC	TAC	TAA	ACA	GG	-C	G-GA	TA	-T	TAT	
Chimp	CAC	TAA	GCT	CG	---	C	TTT	CTT	GCT	GT	-C	CAA	TTT	CTA	TTA	-	AAG	GTT	CCT	TTG	TTC	GCT	AAG	TCC	AAC	TAC	TAA	ACA	GG	-C	G-GA	TA	-T	TAT	
Rhesus	CAC	TAA	GCT	CA	---	C	TTT	CTT	GCT	GT	-C	CAA	TTT	CTA	CCA	-	AAG	GTT	CCT	TTG	TTC	CCA	AAG	TCC	AAC	TAC	TGA	ACA	GG	-C	G-GA	TA	-T	TAT	
Tarsier	---	---	---	---	---	---	---	---	---	---	---	---	---	---	---	---	---	---	---	---	---	---	---	---	---	---	---	---	---	---	---				
Mouse_lemur	CAC	TGA	GCT	CC	---	C	TTT	CTT	GCT	GC	-C	CAA	TGC	CTA	TTA	-	AAG	GTC	CCT	TTG	TCC	CCA	GAG	GCC	AAC	TAC	AAA	AGA	TA	-G	G-GA	AG	-T	TAT	
Bushbaby	CAC	TGA	GCT	CC	---	---	TTT	CCT	GCT	AC	-T	GAG	TTC	CTA	TTA	-	AAG	A-C	CCA	GTG	TTC	CCA	GAA	CCT	ACC	TAC	AAA	ACA	CA	-G	A-GA	AA	-T	TAT	
TreeShrew	CAC	TAA	ACT	TT	---	C	TTT	CCT	GCT	GT	-C	CTG	TTC	CTA	T-A	-	AAG	TCT	CCC	CCA	ATA	TCT	GAG	---	---	-AC	CAC	TG	-G	G-GA	AA	-T	GAT		
Mouse	CAC	TAA	GCC	CC	---	T	TTT	C-T	GCT	AT	-T	GTC	TAC	GCA	CAA	-	A-G	GTT	ATA	IGT	CCC	CTA	GAG	AAA	AAC	IGT	CAA	TTG	TG	-G	G-GA	AA	-T	GAT	
Rat	CAC	TAA	ACG	TC	---	T	TTT	CCT	GCT	CT	-T	GTC	TTT	GTG	CAA	-	T-G	GTC	AA	T	TGT	TCC	CAA	GAG	AGC	ATC	TGT	CAG	TTG	TT	-G	TCAA	AA	-T	GAC
Kangaroo_rat	CAC	TGA	GCT	CCCTCCT	TTT	CCT	GCT	AC	-C	TGC	TTT	CTA	TTA	-	AAG	GTT	CC	TTA	TCC	CCA	AAG	AAC	ATC	TAC	CAA	ATA	TG	-G	GGAA	AA	-T	CAT			
Guinea_Pig	CAC	TGA	ACA	TT	---	C	TTT	TC	GCC	AC	-C	CAC	CTC	TTG	AGG	-	GAG	GTT	TCT	CTG	TCC	GCT	GAG	AAC	AAC	TAC	TAA	ATA	CA	-G	GGGA	AA	-T	TAT	
Squirrel	CAC	TAA	GCT	AC	---	C	TTT	CCT	GCT	AC	-C	TAT	CTC	ATA	CAA	-	AAG	GC	-CT	TTT	TCC	CCA	GAG	AAC	AAC	TAC	TAA	ATA	TT	-G	GGGA	AC	-T	TAT	
Rabbit	CAC	TGA	CAT	---	---	---	---	---	---	---	---	---	---	---	---	---	---	---	---	---	---	---	---	---	---	---	---	---	---	---	---				

Figure S11. Estimated extent of readthrough in *C. elegans* using comparative evidence.
 Frequency (y-axis) of PhyloCSF scores per codon (x-axis) for *C. elegans* second ORFs in three frames. In contrast to the similar analysis for *D. melanogaster* (Figure 5A) no significant excess is found in frame 0, suggesting lack of abundant readthrough in *C. elegans*. Scores of five readthrough candidates found by manual curation are indicated with stars.

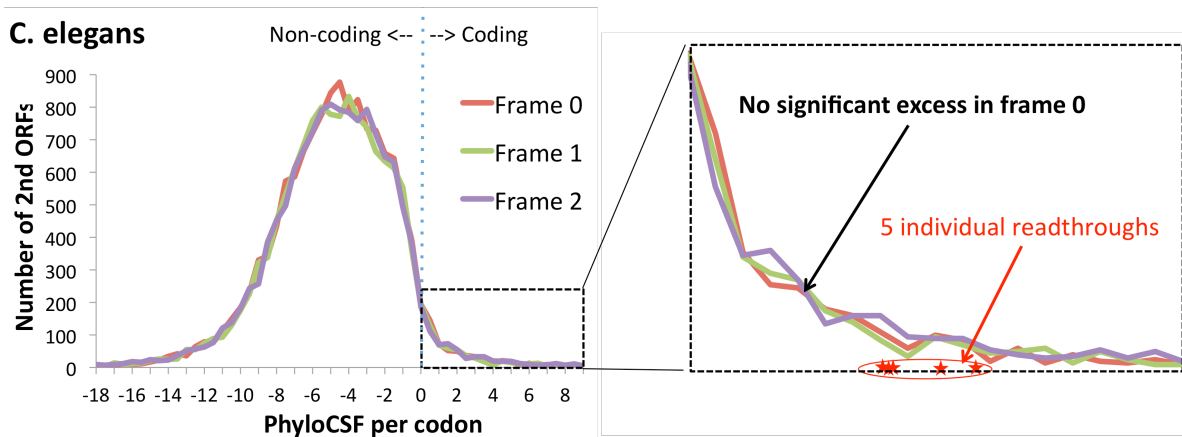


Figure S12. GFP images with controls. GFP images of the readthrough strains shown in Figure 3B matched to wildtype embryos or larva with similar development stage and orientation ($y^1; cn^1 bw^1 sp^1$ strain). Although some staining is seen in the control images, it is neither as bright nor as specific as in images of the readthrough strains.

